JGR Planets

RESEARCH ARTICLE
10.1029/2022JE007241

Key Points:

- For the first time after 5 years, we show a global picture of the North polar cyclones' structure, which has remained almost unperturbed
- Each cyclone has a peculiar morphology, which differs from the others and it is stable over the observed lapse of time
- Beta-drift is not responsible for the motion of the vortices on timescales of months

Supporting Information:

Supporting Information may be found in the online version of this article.

Correspondence to:

A. Mura,
alessandro.mura@inaf.it

Citation:

Mura, A., Scarica, P., Grassi, D., Adriani, A., Bracco, A., Piccioni, G., et al. (2022). Five years of observations of the circumpolar cyclones of Jupiter. *Journal of Geophysical Research: Planets*, *127*, e2022JE007241. https://doi.org/10.1029/2022JE007241

Received 9 FEB 2022
Accepted 26 AUG 2022

Author Contributions:

Conceptualization: A. Mura, A. Bracco, A. Ingersoll
Data curation: A. Mura, P. Scarica
Formal analysis: A. Mura
Investigation: A. Mura, P. Scarica, D. Grassi, A. Adriani, A. Bracco, G. Piccioni, G. Sindoni, M. L. Moriconi, C. Plainaki, A. Ingersoll, F. Altieri, A. Cicchetti, B. M. Dinelli, G. Filacchione, A. Migliorini, R. Noschese, R. Sordini, S. Stefani, F. Tosi, D. Turrini
Methodology: A. Mura
Project Administration: A. Mura
Resources: A. Mura
Software: A. Mura
Supervision: A. Mura

Five Years of Observations of the Circumpolar Cyclones of Jupiter

A. Mura[1], P. Scarica[1], D. Grassi[1], A. Adriani[1], A. Bracco[2], G. Piccioni[1], G. Sindoni[1], M. L. Moriconi[3], C. Plainaki[4], A. Ingersoll[5], F. Altieri[1], A. Cicchetti[1], B. M. Dinelli[3], G. Filacchione[1], A. Migliorini[1], R. Noschese[1], R. Sordini[1], S. Stefani[1], F. Tosi[1], and D. Turrini[1]

[1]INAF–Istituto Nazionale di Astrofisica, Roma, Italy, [2]Georgia Institute of Technology, Atlanta, GA, USA, [3]CNR–Istituto di Scienze dell'Atmosfera e del Clima, Bologna, Italy, [4]Agenzia Spaziale Italiana, Roma, Italy, [5]California Institute of Technology, Pasadena, CA, USA

Abstract The regular polygons of circumpolar cyclones, discovered by Juno in 2017, are one of the most puzzling features of Jupiter. Here we show new recent global pictures of the North polar cyclones' structure. These are the first simultaneous images of the whole structure since 2017, and we find that it remained almost unperturbed, just like the South one. The observation of these long-lasting structures poses questions regarding the formation mechanism of cyclones, and on their vertical structure. Data by Juno/JIRAM infrared camera collected over the last 5 years show that cyclones migrate around what may seem like equilibrium positions, with timescales of a few months but, aside from that, the cyclones systems are very stable. Our analysis of the observations shows that the motion of cyclones around their equilibrium position is uncorrelated with their position if a barotropic approximation (β-drift) is assumed. Thus, a different dynamical explanation than the barotropic β-drift is needed to explain the stability of the observed features. Each cyclone has a peculiar morphology, which differs from the others and is stable over the observed lapse of time in most cases.

Plain Language Summary In 2017, Juno discovered that the poles of Jupiter are occupied by regular polygons of cyclones. Here we report 5 years of observations of these cyclones by JIRAM, the infrared imaging spectrometer on board Juno. In particular, we show the latest observations of the North Pole cyclones structure. In fact, this structure has only been partially observed since its discovery 5 years ago. One important question is how these structures of cyclones form, and if they are stable. We find that both remained almost unperturbed. Hence, we show that these cyclones may have very long lifetimes. Cyclones migrate around what may appear to be equilibrium positions. The scale time is a few months. We analyzed the movement of cyclones and compared it with a model where winds don't change with depth (a barotropic model). We found that the motion of the cyclones is not related to their position according to this model. We conclude that a different model is needed to explain some of the observed characteristics. Each cyclone has a peculiar morphology, which differs from the others and is stable over the observed time span in most cases.

1. Introduction

The NASA/Juno mission (Bolton et al., 2017, 2018) discovered the existence of Jupiter's circumpolar cyclones in February 2017 (Adriani et al., 2018, 2020), when observing the poles for the first time after orbit insertion. The observations were made possible by JIRAM (Jovian InfraRed Auroral Mapper, Adriani et al., 2017) and JunoCam (Hansen et al., 2017). JIRAM, in particular, being an infrared camera, can follow the evolution of these structures in any illumination condition and has monitored them since 2017 (Mura et al., 2021).

The North Pole region is occupied by a Polar Cyclone (PC) surrounded by eight Circum-Polar Cyclones (CPCs) while the South Pole is populated with five cyclones surrounding a polar one. Adriani et al. (2018) reported that the South CPCs have approximately the same size as the South PC, while North CPCs are, on average, smaller than the North PC. Mura et al. (2021) reported three characteristics of these PCs and CPCs observed over 4 years. First, all the cyclones in the structures are very long-living and stable: at that time, they estimated that the lifetime should be longer than 20 years. Second, the structures formed by the CPCs rotate very slowly, with the North and South ones having substantially different rotation speeds (3° and 7° per year, westward, respectively). Finally, the cyclones are subjected to oscillations that propagate from one to the other and have timescales of the order of a few months.

Validation: A. Mura
Visualization: A. Mura
Writing – original draft: A. Mura, A. Bracco
Writing – review & editing: A. Mura

Within the structure formed by the CPCs, small anticyclonic vortices are often observed, both at the North and at the South Pole. These anticyclones are often less than 1,000 km in size, as discussed in Adriani et al. (2020). For cyclones, tangential speeds increase starting from the center up to a maximum of about 1,000 km, where typical values of 50–100 m/s are reached, depending on the specific cyclone considered, while the smaller anticyclonic eddies also have lower velocities (Grassi et al., 2018). In this study, we do not discuss anticyclones, but instead, we focus on the stability and instability of the position of the larger cyclones.

A very brief summary of the many existing models, that can be useful to explain their stability or their genesis, is given in Mura et al. (2021). They classify these models into two broad classes: "deep" (i.e., Cai et al., 2021; Garcia et al., 2020; Heimpel et al., 2005, 2016) and "shallow" (i.e., Gavriel & Kaspi, 2021; Li et al., 2020; Reinaud, 2019; Reinaud & Dritschel, 2019).

In convective deep models, the cyclones are generated in the surface mixed-layer under the influence of deep convective plumes that are rooted deeply into the Jovian atmosphere and exchange heat from the inner part to the base of the mixed-layer. In shallow models, the surface forcing is responsible for the formation of vortices in approximate geostrophic balance, therefore characterized by a weak vertical velocity field (compared to the horizontal one).

Among convective models, we just note that a recent model by Siegelman et al. (2022), not discussed in our previous work, showed that at scales of the order of 100 km or less, turbulence at the Jupiter poles is dominated by shallow convective instabilities that can feed energy to the much larger cyclones.

Among shallow models, studies have been performed either allowing for (small) vertical accelerations and assuming that the vertical scale of the turbulent flow is far smaller than the horizontal one, or using the barotropic approximation, where the vertical velocity field is constant and vertical accelerations are null. For example, Reinaud (2019) and Reinaud and Dritschel (2019) tried to explain the stability of the overall PC-CPC structures using the quasi-geostrophic approximation but did not account for the change in Coriolis parameter as the latitude varies, the so-called beta-effect, which is responsible for the drift of cyclonic eddies toward the Pole and may affect stability. The beta-effect was taken into account by Li et al. (2020), who seeded a given number of (shallow) cyclones in a shallow-water model. Li et al. (2020) were able to reproduce the poleward drift and the grouping into regular polygonal patterns that are stable whether the shallow layer hosting them is not too thin or too deep and only if each cyclone is shielded by an anticyclonic ring of vorticity. Finally, the work by Gavriel and Kaspi (2021) uses a barotropic model to explain the presence of regular polygons of cyclones at the poles of Jupiter, and why they should not form at Saturn.

For simplicity, in this study, by "deep" we mean convective and by "shallow" we mean both shallow water vortices but also barotropic vortices that extend vertically but are generated by processes that are evident on the surface.

JIRAM data can be used to test the validity and accuracy of these models. For example, the model by Li et al. (2020) requires a mean, stable field of anti-cyclonic winds between cyclones to ensure their shielding and therefore their stability. Grassi et al. (2018), calculated the wind field in the polar regions by using multiple images of the same regions separated by a short time scale, and from the wind field, it is possible to calculate the vorticity distribution map and infer how cyclones should move. In Mura et al. (2021) we presented an analysis of the first 4 years of JIRAM observations, focusing on the secular variations. Here we add new data from the fifth year of JIRAM images, and use the observations and wind estimations to test predictions from a barotropic model.

2. Data

JIRAM recorded images of South polar cyclones almost every close passage of Juno (PeriJove, PJ). PeriJoves occurred with a period of 53 days until PJ 34 (June 2021), after which the period shortened. The coverage of the North pole, on the other hand, is less regular (see Table 1 and Table 2). After almost 5 years of observation, very little has changed in the polar cyclones structures. In the South, as described in Mura et al. (2021), the pentagonal structure did not change substantially, only occasional perturbations have been observed. An important observation, which required a special turning of the spacecraft's rotation axis, shows that the North polar cyclone structure is almost unperturbed after 5 years (see Text S1–S3 in Supporting Information S1). The octagonal structure in the North is still present: Figure 1, panel B, shows the eight North CPCs, which make a less regular polygon

Table 1
Summary of South Pole Observations

PJ	Date	Lat 1	Lat 2	Lat 3	Lat 4	Lat 5	Lat SP	Lon 1	Lon 2	Lon 3	Lon 4	Lon 5	Lon SP
4	02/02/2017	83.7	84.3	85.0	84.1	83.2	88.6	157.1	94.3	13.4	298.8	229.7	211.3
5	03/27/2017	83.0	84.3				87.8	160.9	103.4				203.1
6	05/19/2017	83.1	84.7	85.5	84.1	82.3	87.6	160.3	102.2	11.9	289.0	234.4	213.9
8	09/01/2017	83.6	85.2	85.4	83.4	82.4	87.8	160.4	93.1	12.4	302.3	248.1	238.1
9	10/24/2017	83.8	84.8	84.9	83.4	82.9	88.5	167.9	97.6	12.4	305.1	250.3	239.1
11	02/07/2018	83.2	84.1	84.7	84.3	83.1	88.5	167.8	106.6	28.5	304.1	240.2	215.0
13	05/24/2018	83.1	84.7	85.8	84.1	82.5	88.1	173.6	114.1	27.4	301.5	245.8	222.3
14	07/16/2018	83.5	85.1	85.2	83.7	82.6	87.9	178.2	111.8	17.3	303.0	245.5	232.8
15	09/07/2018	84.4	85.0	84.7	83.4	82.6	88.0	174.2	104.0	18.7	306.2	238.9	250.8
17	12/21/2018	83.5	84.5	84.9	83.9	82.8	88.3	170.5	107.6	29.9	309.4	251.4	225.8
18	02/12/2019	83.3	84.4	85.5	84.3	82.7	87.8	170.9	112.1	32.7	316.1	260.1	224.4
19	04/06/2019	83.1	84.5	85.5	84.0	82.8	87.7	176.4	119.5	31.1	316.2	259.5	230.3
20	05/29/2019	83.4	84.6	85.1	83.9	82.9	88.0	183.7	119.6	35.4	317.8	256.6	242.3
21	07/21/2019	84.0	84.8	85.4	83.5	82.5	87.9	182.7	118.9	33.3	318.0	259.4	250.5
22	09/12/2019	83.8	84.8	85.2	83.8	82.8	88.2	176.9	116.9	31.2	319.4	264.0	245.4
23	11/03/2019	83.0	84.6	85.8	83.9	83.1	88.0	168.0	110.6	32.8	318.2	263.5	224.3
24	12/26/2019	82.8	84.3	85.5	84.3	83.3	87.9	175.2	117.6	33.5	316.5	259.0	217.5
25	02/17/2020	83.1	84.6	85.5	84.1	82.7	88.0	186.3	123.0	35.7	312.6	247.0	234.8
26	04/10/2020	83.7	84.8	85.8	83.7		87.3	185.9	126.2	33.1	318.1		254.4
27	06/02/2020	84.1	84.8		83.3	82.2	87.3	190.8	119.7		323.9	252.4	269.5
28	07/25/2020	84.2	85.3	84.9	83.2	82.8	87.9	190.8	124.9	31.2	323.1	250.2	270.2
30	11/08/2020	83.8	84.4	85.0	83.9	83.0	88.6	185.0	122.3	47.8	327.3	255.5	258.7
31	12/30/2020	83.0	84.3	85.0	84.6	83.3	88.2	184.7	126.6	48.1	327.4	264.4	232.1
32	02/21/2021	83.1	84.0	86.0	84.4	82.6	87.5	186.6	128.6	54.4	323.6	270.2	235.0
33	04/15/2021	82.9	84.2	86.1	84.3	82.1	86.8	190.7	133.4	53.3	324.2	274.6	240.3
34	06/08/2021	83.5	85.0	86.1	83.2	82.3	87.7	196.8	133.9	35.1	328.4	272.7	256.1
35	07/21/2021	83.4	85.0	85.6	83.8	82.4	87.8	196.2	126.3	36.8	331.9	261.3	260.1
36	09/02/2021	84.0	85.0	84.7	83.7	83.0	88.2	198.2	126.0	45.1	327.5	270.8	266.5
37	10/16/2021	84.1	84.7	84.6	83.3	83.4	88.7	196.8	130.6	46.1	337.2	274.6	277.0
38	11/29/2021	83.5	84.6			82.9	88.3	197.9	135.0			287.1	252.6
39	01/12/2022	83.5	84.4	84.9	83.5	82.7	87.9	203.5	147.4	65.7	351.9	294.5	262.8

Note. Central cyclone close to the South pole is named "SP", latitudes are planetocentric. Longitudes are W.

during the latest pass (29 November 2021), but still clearly recognizable; panel A shows the initial configuration as seen in 2017 (Adriani et al., 2017). Figure 2 shows similar images of the South pole in February 2017 and November 2021; the persistence of the 5-cyclones structure around the PC is less surprising because continuous observations of this feature are available since 2017.

A notable feature in Figure 2 is the appearance of a small cyclone in the same position of that reported by Mura et al. (2021), that is, halfway between CPC1 and CPC5 (close to 250°W in this figure). This is quite surprising, because one could expect that "intruders" could appear in any of the five gaps between the CPCs. By analyzing images of previous orbits, it appears that another small cyclone was also observed in a similar location during PJ9 (October 2017) (Figure S1 in Supporting Information S1).

In Table 1 we present the sequence of all observations of the South Pole from 2017 to today, as an update to Table 1 in Mura et al. (2021), showing latitudes and longitudes of cyclones; Table 2 is for the North Pole. Until PJ34

Table 2
Summary of North Pole Observations

PJ	Lat 1	Lat 2	Lat 3	Lat 4	Lat 5	Lat 6	Lat 7	Lat 8	Lat NP	Lon 1	Lon 2	Lon 3	Lon 4	Lon 5	Lon 6	Lon 7	Lon 8	Lon NP
4	82.9	83.8	82.0	83.2	82.9	83.2	82.3	83.5	89.6	1.4	50.7	95.3	137.6	183.4	227.6	269.9	314.8	230.4
5					83.1	83.2	81.8							179.7	227.3	269.7		
6	83.2	83.7	82.0	83.2	82.8	83.1	81.9	83.3	89.9	359.0	50.2	95.5	136.6	183.6	226.5	271.8	311.8	193.0
9	82.6		83.1	83.4	83.2	83.8	82.1	83.4		359.3		89.8	135.0	179.9	227.5	268.0	312.6	
10			82.3				82.1		89.5			93.7				271.1		107.8
14		83.2			83.2	84.2					53.0			194.0	244.6			
16	82.8		82.7	82.7		83.9	81.6		89.4	6.4		100.4	147.6		244.2	285.1		118.2
24		83.1				83.8			90.0		59.6				235.5			211.0
26	83.2	83.4	82.8	82.5	82.7				89.8	7.0	56.3	102.0	143.6	190.4				240.5
28	83.2	83.1	82.3							9.0	58.2	104.2						
32	83.2								89.1	7.5								131.2
33	83.1		83.0	82.9				85.2	89.0	7.7		110.1	153.7				317.2	160.9
34	83.0	83.8	82.8	82.8	83.2	83.8	81.4	85.6	88.8	10.3	60.8	109.3	156.3	204.1	249.3	294.4	326.5	139.0
35	83.0	83.8	83.3	82.9		83.8		85.5	88.9	11.5	63.1	113.4	158.6		255.0		322.8	164.2
36	82.9				83.1			85.3	89.1	13.2				208.0			325.4	146.2
37	82.9				83.4				89.1	14.9				206.4				137.4
38	82.8	83.0	82.4	82.9	83.5	84.5	81.8	84.8	89.1	18.7	65.5	111.5	155.3	205.2	252.7	295.1	331.1	122.4

Note. Central cyclone close to the North pole is named "NP", latitudes are planetocentric. Longitudes are W.

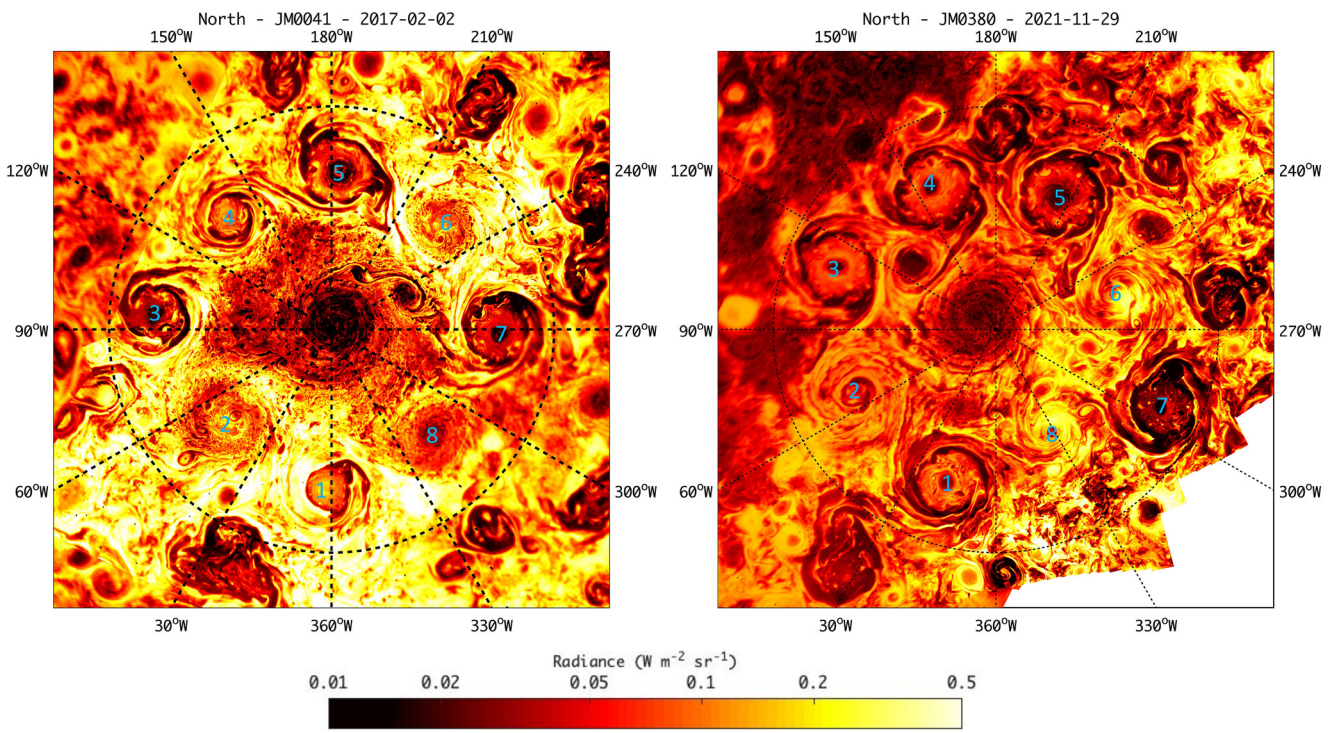

Figure 1. Comparison between North structure in Feb. 2017 (left) versus Nov. 2021 (right). circumpolar cyclones are indicated by cyan numbers. The pseudo-color maps show band radiance in the M band (4.5–5 μm). The circle is the 80° N parallel, latitudes are planetocentric. The lower average radiance in the observations of November 2021 is due to a residual of the correction due to the emission angle. The whole structure rotated approximately 15° westward between the two observations.

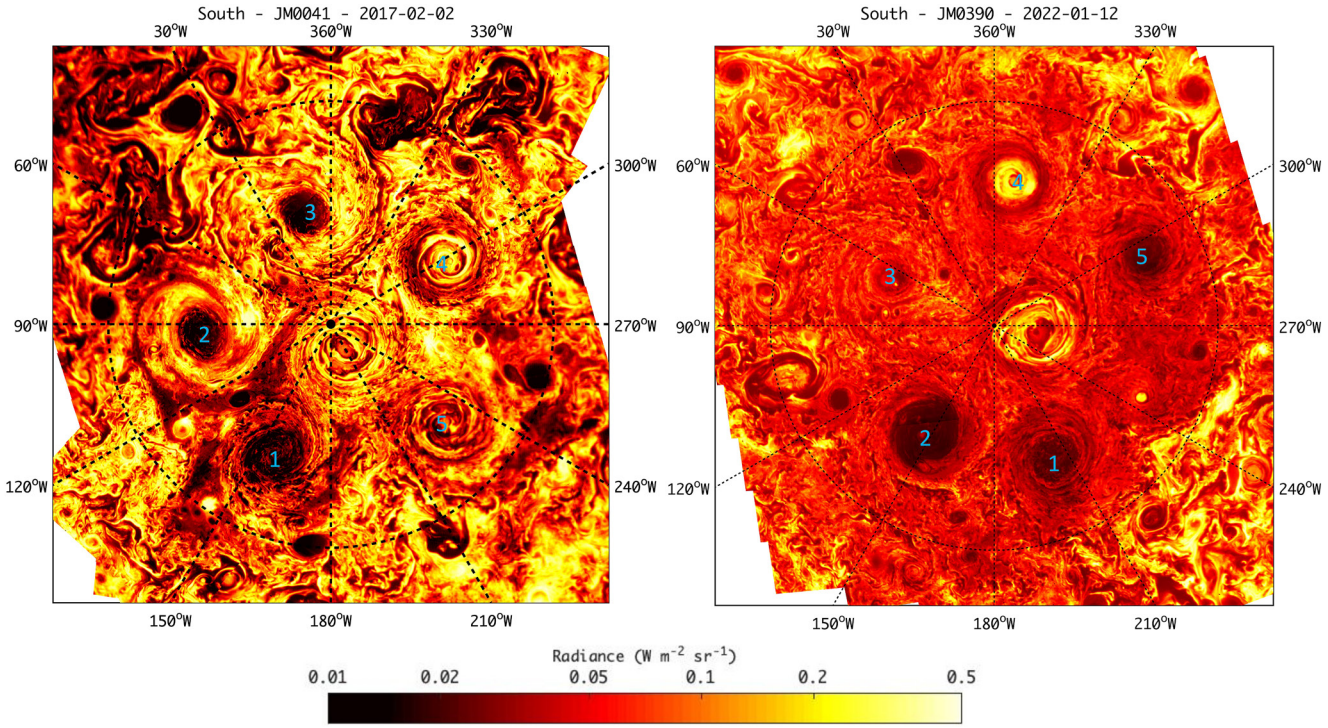

Figure 2. Comparison between South structure in February 2017 (left) versus January 2022 (right). circumpolar cyclones are indicated by cyan numbers. The pseudo-color maps show band radiance in the M band (4.5–5 μm). The circle is the 80°S parallel, latitudes are planetocentric. The whole structure rotated approximately 30° westward between the two observations.

(June 2021), Juno's orbit period was about 53 days; from PJ34 on, the orbit period was reduced to about 43 days; therefore, these are the minimum time intervals between two successive observations reported here. Similar to the previous observations, the spatial resolution at the reference level of 1 bar ranges approximately from 15 to 60 km. The average drift velocity (in absolute value), obtained from Table 1, is between 0.1 and 0.2 m/s, with no significative difference, on average, between cyclones. The position of the center of the cyclones cannot be determined with automatic recognition software (the morphology of cyclones differs from cyclone to cyclone, as discussed later) and therefore has been identified manually. These observations confirm the oscillation patterns already identified in the previous work.

Single cyclones have peculiar morphology in IR images. Some are darker (colder) with curly patterns, others are brighter, with large and clear high-contrast features. Comparable morphological differences can be found in the surface expression of ocean mesoscale eddies simulated at submesoscale permitting resolution (1 km or higher). In the oceanic analog differences are generally attributable to changes in mixed-layer depths (see e.g., Figure 4 in Liu et al. (2021) noting that for this basin, anticyclones are the norm). Often, the morphology of Jupiter PCs is still recognizable after 5 years. In Figure 3, we show examples of 4 cyclones' morphology observed almost 5 years apart. It appears that cyclones' shapes always fall in one of three types. Type 1 (left column) shows a few large branches with almost no small features; North CPC5 is an example. Type 2 (second and third columns) cyclones are very cloudy, with curly branches very rich in smaller features. In this type, the cyclone's eye is round and darker. Type 3 cyclones (right column) show alternating cloudy and cloudless rings, with an oval eye. This morphologic aspect is not a parameter that can be easily quantified and used to feed a model, but it is however suggestive of a tendency of cyclones to maintain their characteristics over a long time.

However, some exceptions to this scheme are evident. The most notable one is South CPC4 which displayed a sudden change in brightness and morphology on a very short time scale. In Figure 4 we show five images of South CPC4 taken ~2 months apart. It appears that this cyclone, which has usually a cloudy core, like South CPC1, has become darker until PJ32, and suddenly became extremely bright, with a cloudless core (PJ33). Later on, it seemed to slowly recover its initial morphology (PJ34, 35, and 36). The reason for this event, so far, has no clear explanation (it is reported here mostly because no other cyclone ever showed a similar behavior). It will be

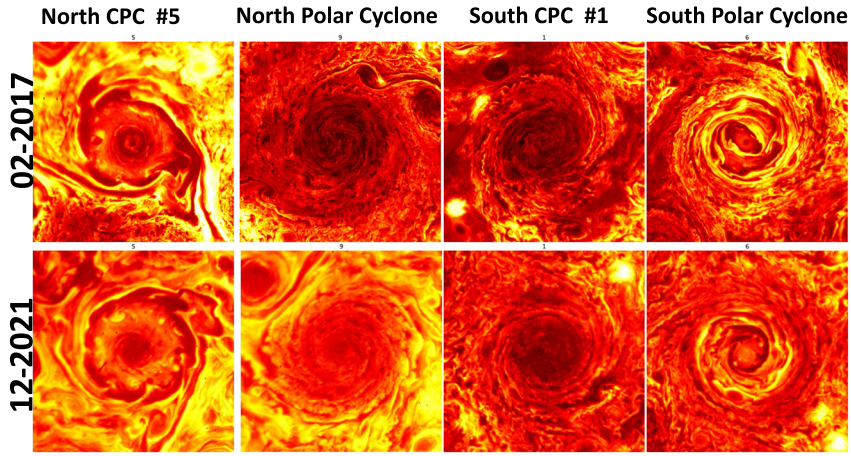

Figure 3. Three examples of cyclones morphology. Type 1 (left column): few large branches with almost no small features. Type 2 (second and third columns): cloudy cyclones, with curly branches, very rich in features, with round cyclone's eye. Type 3 (right column): alternating cloudy and cloudless rings, with an oval eye. Each panel shows a region 8,000 × 8,000 km wide. The pseudo-color maps show band radiance in the M band (4.5–5 μm), same scale as Figures 1 and 2.

extremely important to observe the evolution of this cyclone in the future, to understand if it remains stable in a configuration similar to the initial one, or it experiences other sudden changes. It is also worth noting that this is probably the event with the shortest time scale in the dynamics of CPCs, since drifts usually occur over the timescale of several (∼6) months, and the appearance of a temporary sixth CPC in the South pole, reported in Mura et al. (2021), also occurred over a similar period.

There is another interesting feature in the images of CPC4: as soon as the whole cyclone became very bright, two small cyclonic features appeared inside the core. It is worth noting that these two small cyclones lasted for at least 7 months. That is, small features inside cyclones cores are more stable than larger features outside them: as reported by Adriani et al. (2020), small features outside the cyclones are merged and destroyed very easily.

3. Lifetime of Cyclones

As discussed in Mura et al. (2021), it is difficult to estimate the cyclone's lifetime, or the probability of creation of new stable cyclones, since we do not have any such occurrence. As in Mura et al. (2021), assuming that these 15 cyclones have a similar lifetime τ, the probability for 15 cyclones to be all alive after n years is:

$$p = e^{-15n/\tau}$$

because it is the product of the probability of no "disappearance" for 15 cyclones after n years (each is $e^{-1/\tau}$). If we already observed no "disappearances", then $p(\tau)$ is also the likelihood, which is function of the model parameter τ (assuming $n = 5$). The likelihood increases from 0 ($\tau = 0$) to 1 for very long τ (i.e., a very long τ passes a likelihood test). Any τ less than ∼70 years fails a 1-sigma likelihood test (i.e., it has a small likelihood: $p < 0.32$); and

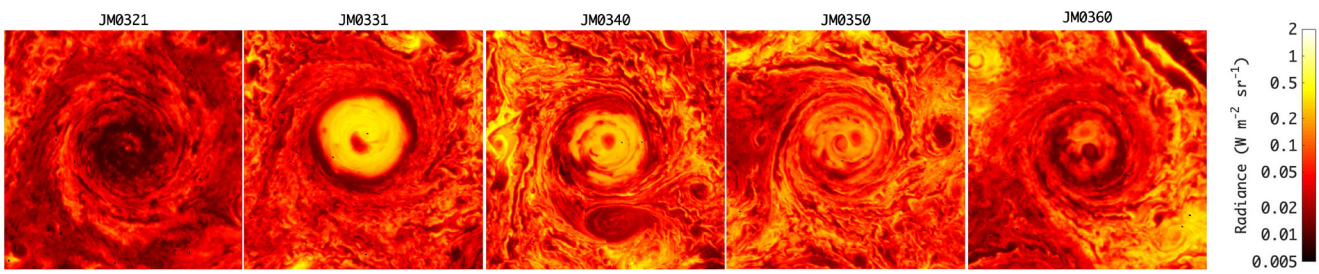

Figure 4. The evolution of South circumpolar cyclones 4 from orbit 32 (*JM0321*) to orbit 36 (*JM0360*). Date are (from left to right): 12/30/2020; 02/21/2021; 04/15/2021; 06/08/2021; 07/21/2021. Each panel shows a region 8,000 × 8,000 km wide. The pseudo-color maps show band radiance in the M band (4.5–5 μm), with a different scale with respect to Figures 1–3, to enhance the morphology of the inner part of the cyclone.

any τ less than ~25 years fails a 2-sigma likelihood test (i.e., it has an extremely small likelihood: $p < 0.05$). In summary, τ is likely longer than ~70 years, and surely longer than ~25.

Note that this formula assumes vortices that behave independent of each other, and that could be a doubtful hypothesis if the vortices are linked dynamically. However, we already have an example when the South system moved from a "5 + 1" to a "6 + 1" configuration, for almost 6 months, and then getting back to a "5 + 1" configuration, so that, relying on observations only, it seems a fair assumption that the appearance/destruction of a large cyclone nearby does not affect the others very much. But, indeed, if we assume that the lifetime of a cyclone is dependent on of the others, then it is not possible to say much about the expected lifetime of these cyclones, from observations.

4. Stability of Cyclones

For Jupiter, the poleward drift of cyclones due to the gradient of the vorticity field has been suggested by Li et al. (2020), and Gavriel and Kaspi (2021). The latter study, in particular, assumes a barotropic model for the cyclones in which the large-scale movement of vortices is due, to the first order, to advection of the background vorticity with the tangential velocity of the vortex. By using this simple vorticity model the authors could reproduce the stability of Jupiter CPCs and show why Saturn has no stable CPCs. This is a consequence of the different planetary radius and angular velocity between Jupiter and Saturn, and of the different size and tangent velocity of the respective PCs. It is a different approach with respect to O'Neill et al. (2015, 2016) and Brueshaber et al. (2019), who found that the planetary Burger number (B_u) is a key quantity that leads to different polar dynamical regimes ($B_u = {L_d}^2/a^2$, with a the radius of the planet, and L_d the radius of atmospheric deformation). Gavriel and Kaspi (2021) also estimate the number of cyclones and equilibrium latitude. In this paper, we adopt the same theoretical framework, with emphasis on the South PC-CPCs system, since we have much more data (see also Text S1–S3 in Supporting Information S1).

The initial condition is the rest position for the cyclones, and the only two relevant parameters that need to be estimated are the radius (R) and tangent velocity at R (V) of all cyclones, which we derive from JIRAM observations; the planetary vorticity and vorticity gradient are known. In Gavriel and Kaspi (2021), the velocity field is a piecewise function that linearly increases up to R, and then it decreases exponentially. We note that using the same method, we do not find exactly the same equilibrium latitude and number of cyclones. One reason for this discrepancy is that we use the best fit (minimizing the chi-square) of the data from Grassi et al. (2018), (see Text S1–S3 in Supporting Information S1) to obtain R and V, while values in Gavriel and Kaspi (2021) are assumed (but not fitted) from Figure 6 of Grassi et al. (2018). Additionally, while Gavriel and Kaspi (2021) used a multiplicative factor of 1/0.75 for R (South CPCs only), to account for the fact that the South CPCs could be larger than the South PC (Figure 6b in Adriani et al., 2020), we prefer not to make this assumption, as Adriani et al. (2020) concluded that it is the North PC to be larger than North CPCs, rather than the South CPCs being larger than the South PC. We then calculate the meridional equilibrium (Equation 1 in Gavriel & Kaspi, 2021) and we find that the equilibrium latitudes are 83°40′S and 84°20′N. At these latitudes, by using Equation 2 in Gavriel and Kaspi 2021 study, it is possible to fit eight and ten cyclones in the South and North hemispheres, respectively. However, once all these CPCs are grouped, the system is not in an equilibrium condition anymore, because there is an extra repulsion "force" exerted on a CPC by the two surrounding CPCs (the two forces nullify in the zonal direction but not in the meridional direction) and the equilibrium latitude shifts equatorward. We iterate until both meridional and zonal equilibrium are satisfied and we find that the number of cyclones gets much larger than observed: 11 and 15. This discrepancy alone does not imply that the model has problems, since the two parameters R and V have large uncertainties, which are of the order of 10%–20%. Also, the above calculation assumes that all CPCs have the same R and V of the relative PC, and the validity of this assumption should be checked. One could also use the velocity field of other cyclones (Grassi et al., 2018, gave only the velocity field along with an x and y cut of the central cyclones). To avoid the impasse, since the number n and latitude L of cyclones are two established parameters, it is possible to estimate V and R that provide the correct values of n and L: V should be 85 m/s and R should be 1,300 km and 1,800 km (North and South respectively). The uncertainty, when estimating R in this way, is of the order of 100 km.

A robust test for a barotropic model that takes into account the beta-drift is to examine whether it shows some correlation with the observed cyclone motions around their rest position. If we take the positions of the cyclones at a two given Juno PeriJoves epoch t_i *and* t_{i+1}, and we estimate the expected drift direction (see Text S1–S3 in

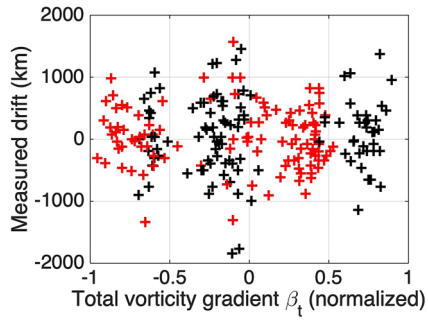

Figure 5. Scatterplot of the measured drift of cyclones (*y* axis) versus the total gradient of vorticity (*x* axis, normalized units) for the South hemisphere. Black and red crosses refer to the *x* and *y* components in System III reference frame, respectively.

Supporting Information S1), we can check if there is a correlation between the observed shift.

Figure 5 shows a scatterplot for this test, using data of the South CPCs only. Each cross in the figure represents the movement of one cyclone from PJ_i to PJ_{i+1}. On the *x* axis we report the calculated gradient of vorticity (so called beta effect) and on the *y* axis the measured drift (in km). Black crosses and red crosses refer to different components in System III reference frame (black: *x* component; red: *y* component). In Text S1–S3 in Supporting Information S1, we describe the calculation of the gradient of vorticity (beta effect). No correlation can be seen between the beta effect and observed cyclone motion. The correlation does not improve by changing *R* and *V*, or even if we include any arbitrary tilt to take into account that cyclones in the South hemisphere don't drift poleward, but rather in the South-West direction (Smith, 1993; see Text S1–S3 in Supporting Information S1 for a list of model runs); the covariance values remain always smaller than 0.2. Hence, under the assumption that all cyclones at the South pole have similar radial profile, their relative motion cannot be explained by this barotropic model. There remains the possibility that each cyclone has its peculiar velocity profile, that substantially differs from the analytical profile we have assumed.

5. Discussion

The observation of long-lasting CPCs poses questions regarding the formation mechanism and whether these cyclones are deep or shallow structures. Some indications that they may be deeply rooted in the Jovian atmosphere have been anticipated in our previous work (Mura et al., 2021), together with a discussion of the most recent theories on cyclones formation (Boury et al., 2021; Reinaud & Dritschel, 2019; Yadav & Bloxham, 2020). Indications were obtained by ascertaining if vortices outside such polar structures, which naturally tend to migrate toward the poles, can easily enter these regular structures and merge with pre-existing cyclones (Li et al., 2020). We found that this is an extremely unlikely event on an annual scale, which has only happened once, and only temporarily. After 5 years, the 8 + 1 North PCs structure and the 5 + 1 South one show very small changes; the lifetime of a single cyclone is therefore longer than 25 years and possibly longer than 75 years. Also, single cyclones have their peculiar morphology and this is often retained after 5 years, both in radiance and in morphology. In particular, this is the first time that we can observe the North CPCs system since the discovery in 2017, and we find that the structure is almost unperturbed, which is a confirmation of the studies by Tabataba-Vakili et al. (2020), and Mura et al. (2021) who also showed that the CPCs remained largely stable over the 2 and 4 years of observations, respectively.

In this study, we show that a barotropic model, based on beta drift only, encounters some problems in explaining the observed features of PCs. In particular, the relative motion of the cyclones has been observed over 5 years: global observations do not show any correlation with the beta effect in terms of drift direction. It is also worth noting that the barotropic approximation of β-drift cannot easily explain the observations described in Mura et al. (2021), who reported that the cyclones move around their rest position with oscillations of ∼6 months of period, with the approximate shape of a sine wave. Such harmonic-like oscillation of a cyclone would be easily explained if the equation of motion of its center is of the type $\ddot{x} = -kx$. The total beta effect is in fact proportional to the distance from rest position ("$-kx$", see Figure 5 panel D in Gavriel & Kaspi, 2021) and it is zero at the rest position. However, in the barotropic model, the cyclones, for most of their lifetime, should be in a condition where the beta effect controls the velocity, and not the acceleration (Smith et al., 1997).

The relative motion of the cyclones is not explained by the beta-drift model when assuming that all cyclones have similar size and radial profile of tangent velocity, which is indeed suggested by the fact that we observe them at the vertices of regular polygons. There remains, however, the possibility that the model could reproduce the observed drift motion with different parameters, varying from one cyclone to another one. The evidence that each cyclone has a different peculiar morphology, which has been conserved over 5 years, reported here, supports this possibility. In summary, we conclude that the observation of cyclone topmost winds fails to explain their motion. Among the many alternatives, there are either different "shallow" models or "deep" models. In the first case, we cite the possibility that an anticyclonic ring, surrounding the cyclones, is providing a shielding, necessary for the

stability of the polygonal pattern (Scarica et al., 2022). This model is supported by the same JIRAM observations of this study, and the key quantity is the retrieved wind field, used to calculate vorticity and divergence fields. In the second case, probably the key quantities from JIRAM observations are the different angular velocity and the different number of cyclones observed at the two Poles, which are suggestive of slightly different Rayleigh number regimes at the two Poles, possibly due to different stratification profiles. This hypothesis may support the suggestions of Cai et al. (2021) that vortices occurring in gas giants form by deep planetary turbulent convection and that, under certain favorable conditions, allows the stability of the configurations.

We report the observations of features that were not reported in our previous study. The first is the recurrent appearance of a small "intruder" cyclone in the same gap, halfway between CPC1 and CPC5. It was reported once by Mura et al. (2021), but here we show two more possible occurrences. The fact that intruders may have a preferred spot is quite difficult to explain in terms of beta effect, also because intruders seem to appear rather than drifting in the gap between CPC1 and CPC5. It is true that our temporal sampling (2 months) can hide some faster movements. At the end of the Juno mission, the period of the orbit will be shortened to 1 month, so that we may have a better understanding of these phenomena.

Then we report the presence of two small cyclones, lasted for at least 7 months, inside the core of CPC4, suggesting that small features inside cyclones cores are more stable than larger features outside them.

Finally, there is a substantial element to consider for a theory of cyclone stability: the evidence that there are few (∼4) different morphological classes into which we can divide the 15 cyclones and that, with very few exceptions, cyclones have the tendency to maintain the same morphology throughout the observation period. This is obviously the most complex parameter to use as an input to a model because it is even difficult to define any quantity from the morphology of the observations. Nevertheless, as cyclone formation and stability models become available and consistent with observations, they can subsequently be tested in light of these morphological properties. While modeling with such level of detail may require significant time and effort, and may not be possible in the immediate future, the observations of these differences among cyclones demonstrate the importance of having a coverage as continuous as possible, at least at the South Pole. Indeed, changes in the morphology of one of the southern cyclones occurred within a time scale of a month.

Conflict of Interest

The authors declare no conflicts of interest relevant to this study.

Data Availability Statement

All data used in this study can be found in Mura (2022). All JIRAM data (Noschese & Adriani, 2017a, 2017b) is publicly available on the Planetary Data System (http://pds.nasa.gov) and can be downloaded from http://atmos.nmsu.edu. The individual datasets are available at https://atmos.nmsu.edu/PDS/data/jnojir_xxxx, where xxxx is 1001, 1002, or 1003 for EDR (Experiment Data Record; raw data) and 2001, 2002, or 2003 for RDR (Reduced Data Record; calibrated data) volumes.

Acknowledgments
This work was supported by the Italian Space Agency (ASI) through ASI-INAF agreement no. 2016-23-H.0 and its addendum no. 2016-23-H.1-2018 and no. 2016-23-H.2-2021. Open Access Funding provided by Istituto Nazionale di Astrofisica within the CRUI-CARE Agreement.

References

Adriani, A., Bracco, A., Grassi, D., Moriconi, M. L., Mura, A., Orton, G., et al. (2020). Two-year observations of the Jupiter polar regions by JIRAM on board Juno. *Journal of Geophysical Research: Planets*, *125*(6), e2019JE006098. https://doi.org/10.1029/2019JE006098

Adriani, A., Filacchione, G., Di Iorio, T., Turrini, D., Noschese, R., Cicchetti, A., et al. (2017). JIRAM, the Jovian infrared auroral mapper. *Space Science Reviews*, *213*(1), 393–446. https://doi.org/10.1007/s11214-014-0094-y

Adriani, A., Mura, A., Orton, G. S., Hansen, C., Altieri, F., Moriconi, M. L., et al. (2018). Clusters of cyclones encircling Jupiter's poles. *Nature*, *555*(7695), 216–219. https://doi.org/10.1038/nature25491

Bolton, S. J., Adriani, A., Allison, M., Anderson, J., Atreya, S., & Wilson, R. (2017). Jupiter's interior and deep atmosphere: The initial pole-to-pole passes with the Juno spacecraft. *Science*, *356*(6340), 821–825. https://doi.org/10.1126/science.aal2108

Bolton, S. J., Lunine, J., Stevenson, D., Connerney, J. E. P., Levin, S., Owen, T. C., et al. (2018). The Juno mission. *Space Science Reviews*, *213*(1–4), 5–37. https://doi.org/10.1007/s11214-017-0429-6

Boury, S., Sibgatullin, I., Ermanyuk, E., Shmakova, N., Odier, P., Joubaud, S., et al. (2021). Vortex cluster arising from an axisymmetric inertial wave attractor. *Journal of Fluid Mechanics*, *926*, A12. https://doi.org/10.1017/jfm.2021.703

Brueshaber, S. R., Sayanagi, K. M., & Dowling, T. E. (2019). Dynamical regimes of giant planet polar vortices. *Icarus*, *1*, 46–61. https://doi.org/10.1016/j.icarus.2019.02.001

Cai, T., Chan, K., & Mayr, H. (2021). Deep, closely-packed, long-lived cyclones on Jupiter's Poles. *The Planetary Science Journal*, *2*, 81. https://doi.org/10.3847/psj/abedbd

Garcia, F., Chambers, F. R., & Watts, A. L. (2020). Deep model simulation of polar vortices in gas giant atmospheres. *Monthly Notices of the Royal Astronomical Society*, *499*(4), 4698–4715. https://doi.org/10.1093/mnras/staa2962

Gavriel, N., & Kaspi, Y. (2021). The number and location of Jupiter's circumpolar cyclones explained by vorticity dynamics. *Nature Geoscience*, *14*(8), 559–563. https://doi.org/10.1038/s41561-021-00781-6

Grassi, D., Adriani, A., Moriconi, M. L., Mura, A., Tabataba-Vakili, F., Ingersoll, A., et al. (2018). First estimate of wind fields in the Jupiter polar regions from JIRAM-Juno images. *Journal of Geophysical Research: Planets*, *123*(6), 1511–1524. https://doi.org/10.1029/2018JE005555

Hansen, C. J., Caplinger, M. A., Ingersoll, A., Ravine, M. A., Jensen, E., Bolton, S., & Orton, G. (2017). Junocam: Juno's outreach camera. *Space Science Reviews*, *213*(1–4), 475–506. https://doi.org/10.1007/s11214-014-0079-x

Heimpel, M., Aurnou, J., & Wicht, J. (2005). Simulation of equatorial and high-latitude jets on Jupiter in a deep convection model. *Nature*, *438*(7065), 193–196. https://doi.org/10.1038/nature04208

Heimpel, M., Gastine, T., & Wicht, J. (2016). Simulation of deep-seated zonal jets and shallow vortices in gas giant atmospheres. *Nature Geoscience*, *9*(1), 19–23. https://doi.org/10.1038/ngeo2601

Li, C., Ingersoll, A. P., Klipfel, A. P., & Brettle, H. (2020). Modeling the stability of polygonal patterns of vortices at the poles of Jupiter as revealed by the Juno spacecraft. *Proceedings of the National Academy of Sciences of the United States of America*, *117*(39), 24082–24087. https://doi.org/10.1073/pnas.2008440117

Liu, G., Bracco, A., & Sitar, A. (2021). Submesoscale mixing across the mixed layer in the Gulf of Mexico. *Frontiers in Marine Science*, *8*, 615066. https://doi.org/10.3389/fmars.2021.615066

Mura, A. (2022). JIRAM CPC. *Zenodo*. https://doi.org/10.5281/zenodo.6792465

Mura, A., Adriani, A., Plainaki, C., Moriconi, M. L., Grassi, D., & Turrini, D. (2021). Oscillations and stability of the Jupiter polar cyclones. *Geophysical Research Letters*, *48*(14). e2021GL094235. https://doi.org/10.1029/2021GL094235

Noschese, R., & Adriani, A. (2017a). JNO-J-JIRAM-2-EDR-V1.0. *NASA Planetary Data System*.

Noschese, R., & Adriani, A. (2017b). JNO-J-JIRAM-3-RDR-V1.0. *NASA planetary Data System*.

O'Neill, M. E., Emanuel, K. A., & Flierl, G. R. (2015). Polar vortex formation in giant-planet atmospheres due to moist convection. *Nature Geoscience*, *8*(7), 523–526. https://doi.org/10.1038/ngeo2459

O'Neill, M. E., Emanuel, K. A., & Flierl, G. R. (2016). Weak jets and strong cyclones: Shallow-water modeling of giant planet polar caps. *Journal of the Atmospheric Sciences*, *73*(4), 1841–1855. https://doi.org/10.1175/JAS-D-15-0314.1

Reinaud, J. N. (2019). Three-dimensional quasi-geostrophic vortex equilibria with m-fold symmetry. *Journal of Fluid Mechanics*, *863*, 32–59. https://doi.org/10.1017/jfm.2018.989

Reinaud, J. N., & Dritschel, D. (2019). The stability and nonlinear evolution of quasi-geostrophic toroidal vortices. *Journal of Fluid Mechanics*, *863*, 60–78. https://doi.org/10.1017/jfm.2018.1013

Scarica, P., Grassi, D., Mura, A., Adriani, A., Ingesrsoll, A., Li, C., et al. (2022). Stability of the Jupiter southern polar vortices inspected through vorticity using Juno/JIRAM data. *Journal of Geophysical Research: Planets*, *127*(8), e2021JE007159. https://doi.org/10.1029/2021JE007159

Siegelman, L., Klein, P., Ingersoll, A. P., Ewald, S. P., Young, W. R., Bracco, A., et al. (2022). Moist convection drives an upscale energy transfer at Jovian high latitudes. *Nature Physics*, *18*(3), 357–361. https://doi.org/10.1038/s41567-021-01458-y

Smith, D. B., Li, X., & Wang, B. (1997). Scaling laws for barotropic vortex beta-drift. *Tellus A: Dynamic Meteorology and Oceanography*, *49*(4), 474–485. https://doi.org/10.3402/tellusa.v49i4.14684

Smith, R. B. (1993). A hurricane beta-drift law. *Journal of the Atmospheric Sciences*, *50*(18), 3213–3215. https://doi.org/10.1175/1520-0469(1993)050<3213:ahbdl>2.0.co;2

Tabataba-Vakili, F., Rogers, J. H., Eichstadt, G., Orton, G. S., Hansen, C. J., Momary, T. W., et al. (2020). Long-term tracking of circumpolar cyclones on Jupiter from polar observations with JunoCam. *Icarus*, *335*, 113405. https://doi.org/10.1016/j.icarus.2019.113405

Yadav, R. K., & Bloxham, J. (2020). Deep rotating convection generates the polar hexagon on Saturn. *Proceedings of the National Academy of Sciences of the United States of America*, *117*(25), 13991–13996. https://doi.org/10.1073/pnas.2000317117

Reference From the Supporting Information

Acton, C. H. (1996). Ancillary data services of NASA's navigation and ancillary information facility. *Planetary and Space Science*, *44*(1), 65–70. https://doi.org/10.1016/0032-0633(95)00107-7